

R. J. Phelan, Jr., and R. H. Rediker, *Appl. Phys. Letters* **6**, 70 (1965).

²J. F. Butler and A. R. Calawa, in *Physics of Quantum Electronics*, edited by P. L. Kelley, B. Lax, and P. E. Tannenwald (McGraw-Hill Book Company, Inc., New York, 1966), p. 458. The results of this paper show that the emission wavelength of the Pb salts corresponds to the energy gap.

³P. M. Nikolic, *Brit. J. Appl. Phys.* **16**, 1075 (1965). Also P. M. Nikolic and J. C. Woolley, private communication.

⁴E. G. Bylander, to be published.

⁵L. Esaki and P. J. Stiles, *Phys. Rev. Letters* **16**, 1108 (1966).

⁶J. B. Conklin, Jr., L. E. Johnson, and G. W. Pratt, Jr., *Phys. Rev.* **137**, A1282 (1965).

⁷F. Herman and S. Skillman, *Atomic Structure Calculations* (Prentice-Hall, Inc., Englewood Cliffs, New Jersey, 1963).

⁸Obtained using a pressure coefficient of the energy gap in PbTe of $-(7.5 \pm 0.3) \times 10^{-6}$ eV/bar (V. Prakash and W. Paul, private communication).

⁹E. G. Bylander and M. Hass, *Solid State Commun.* **4**, 51 (1966).

CRITICAL CURRENTS AND SURFACE SUPERCONDUCTIVITY

J. G. Park

Department of Physics, Imperial College, London, England

(Received 16 May 1966)

In a certain range of magnetic field, metals for which the Ginzburg-Landau parameter κ is greater than 0.417 are superconducting only in regions close to the surface—we suppose the field to be directed everywhere parallel to the surface. Superconductors with $\kappa > 0.417$ include both type-2 superconductors ($\kappa > 0.707$) for which this range of field extends from the upper critical field of the mixed state (H_{C2}) up to the nucleation field for surface superconductivity (H_{C3}), and the class of type-1 superconductor—we shall call them type-1-2 superconductors—for which the range of field runs from the thermodynamic critical field (H_C) up to H_{C3} ($0.417 < \kappa < 0.707$). The three critical fields are related through κ : $H_{C2} = \sqrt{2} \kappa H_C$, $H_{C3} = 1.695 H_{C2}$.¹ In a cylindrical sample whose axis is parallel to the field, the surface superconducting layer forms a hollow cylindrical sheath. Persistent currents induced by the magnetic field as it is changed, inevitably, from one value to another during the measurement of magnetization, at constant temperature, can be expected to flow in this sheath, just as they do in a superconducting tube, and to produce hysteresis effects in the magnetization curve: A hysteretic tail is observed in the magnetization curves of type-1-2^{2,3} and type-2 superconductors⁴; hysteresis due to surface currents is also found in the mixed state of type-2 superconductors.⁵ This type of hysteresis can be distinguished from hysteresis caused in other ways by the form of the minor hysteresis loops and its sensitivity to surface condition. It is brought about because the component of magnetization I pro-

duced by the induced surface currents is diamagnetic when the field is increasing and paramagnetic when it is decreasing. Let us call $|I|$ the surface current magnetization M . See Fig. 1(a).

Fink and Barnes⁶ have recently pointed out that we must expect M for a cylinder in a field parallel to its length to depend on the radius of the cylinder (R) and they have described a method of calculating it. Fink has applied the results of that paper to the calculation of the real and imaginary part of the ac susceptibility.⁷ We have also calculated M , in the same limit ($R \gg \lambda/\kappa$, where λ is the penetration depth), but by a different method which avoids some of the approximations made by Fink and Barnes; our results are in general rather smaller than theirs, particularly for low values of κ when the reduced field h is small ($h = H_0/H_{C2}$ where H_0 is the applied field). In this Letter we describe our calculation of M and also our calculation, by a similar method, of the critical current of a foil carrying a current.

We assume the Ginzburg-Landau equations and the expression for the free energy from whose minimization they may be derived, to describe the behavior of our material. Suppose the surface of the material to be the plane $x = 0$ and the surface current $\vec{j} = (0, j, 0)$ to be everywhere normal to the field $H = (0, 0, H(x))$. We choose a vector potential $\vec{A} = (0, A, 0)$ and write the order parameter ψ in the form

$$\psi/\psi_0 = f(x)e^{iky},$$

where ψ_0 is the order parameter in zero field,

f is a real function of x , and k is assumed to be constant. Substituting in the Ginzburg-Landau equations we have two coupled equations in f and a where $a = A/H_0$:

$$\frac{1}{b} \frac{d^2 f}{dx^2} - b(a-d)^2 f + (f-f^3)/h = 0, \quad (1)$$

$$\frac{d^2 a}{dx^2} - b(a-d)f^2/h\kappa^2 = 0. \quad (2)$$

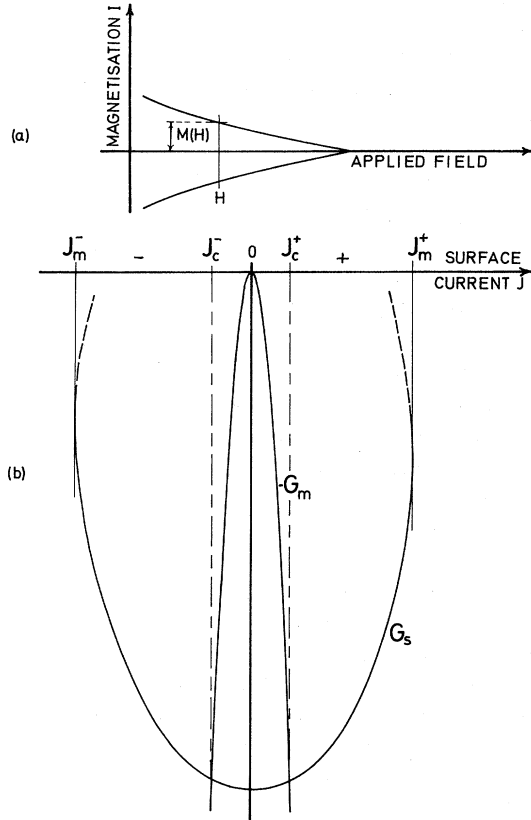


FIG. 1. (a) Hysteretic "tail" on the magnetization curve $I(H_0/H_{C2})$ for a long cylinder in a field H_0 parallel to its length ($H_0 < H_{C3}$) in the range of field where only the surface sheath is superconducting (schematic). $M = |I|$. The origin of applied field is arbitrary. (b) The curves represent schematically the variation with surface current J of the two contributions to the Gibbs free energy of a cylinder radius R : the "surface contribution" $G_s = 2\pi R F_s(J)$, and the "magnetic contribution" $G_m = \pi R^2 F_m(J)$. At the points of intersection of the curves of G_s and $-G_m$, $J = J_c^+$ and J_c^- , respectively, and the free energy of the superconductor carrying a surface current J is equal to that of the normal state (carrying no current). It is assumed that the two branches of the "tail" on the magnetization curve correspond to J_c^+ and J_c^- . J_m^+ and J_m^- are referred to in the text. Solutions of higher free energy than $F_s(J_m^+)$ and $F_s(J_m^-)$ (the dashed curve) are unstable.

In these equations $b = h/\xi^2$ where ξ is the coherence length λ/κ and $d = k\xi^2/h = k/b$. It is convenient to separate the Gibbs free energy G (relative to the normal state) into two terms, i.e., $G = G_s + G_m$. G_m we shall refer to as the magnetic contribution:

$$G_m = \int_v F_m dv, \text{ where } F_m = (H - H_0)^2/8\pi; \quad (3)$$

the integral is taken over the volume of the specimen (v). G_s we shall call the surface contribution:

$$G_s = F_s A, \text{ where } F_s = \xi H_c^2 h^{1/2} \varphi/4\pi; \quad (4)$$

here, A is the surface area of the specimen and φ is a number, obtained after $f(x)$ has been determined, from the following integration:

$$\varphi = \int_0^\infty \left\{ \frac{(df/dx)^2}{b} + b(a-d)^2 f^2 - \frac{f^2(1-\frac{1}{2}f^2)}{h} \right\} b^{1/2} dx.$$

Equation (2) can be rewritten in terms of the current density \vec{j} :

$$\begin{aligned} \vec{j} &= -H_0(5/2\pi\lambda^2)(a-d)f^2 \\ &= -H_0(5b/2\pi\kappa^2h)(a-d)f^2 \text{ A/cm}^2. \end{aligned} \quad (5)$$

Integrating Eq. (1), by parts, with respect to f and combining the result with (5) using boundary conditions $df/dx = 0$ at $x = 0$ and $df/dx = f = 0$ at $x = \infty$, the total surface current per unit width (J) can be related to $f(0)$ and to the other parameters. We define a dimensionless quantity Z by

$$J = Z(5H_c/\pi\kappa\sqrt{2}) \text{ A/cm},$$

in terms of which

$$Z(1 - Z/2\kappa^2h) = [f^2(0)/2h][d^2bh + f^2(0)/2 - 1]. \quad (6)$$

This relation (6) is a generalization of an earlier result which was valid only in the limit of high κ .⁸

In order to find an allowed solution to the differential equations (1) and (2) for certain chosen values of Z , h , b , and κ , $f(0)$ is varied until numerical integration of the equations, starting from $x = 0$ (where we set $df/dx = 0$, $a = 0$, $da/dx = 1$) satisfies the condition $f \rightarrow 0$ and $df/dx \rightarrow 0$ as $x \rightarrow \infty$. The parameter d is obtained from (6). In practice, using a digital computer for the integration, we have usually found $df/dx < 10^{-2}$ at $x = 5$ to be an adequate approximation to the boundary conditions as $x \rightarrow \infty$. Close to H_c , however (or close to H_{c1} for a type-2 superconductor), it is necessary

to integrate to a larger value of x in order to obtain an acceptable solution. In deciding what is acceptable, we are guided by (among other things) a comparison of our chosen value of J with the value obtained for J by integrating (5) using the computed values of f and a .

For any one of the solutions the surface contribution to the free energy per unit area of a plane surface (F_S) varies in the manner shown schematically in Fig. 1(b). At each value of the net surface current J there are usually two allowed solutions; the one of lower free energy is stable—stable in the sense that the free energy (whether the magnetic contribution is included or not) increases with increasing J . The other solution is unstable and will not concern us here.

Consider now a semi-infinite cylinder in a field applied parallel to its length. Our purpose is to calculate the persistent-current magnetization M . We shall assume as Fink and Barnes⁶ did that in the “critical state,” when the maximum persistent current flows, the free-energy difference between superconducting and normal states is $G = 0$. If the radius of the cylinder R is large compared with the thickness of the superconducting sheath ($R \geq 5\xi$), then we can use the value of F_S calculated for a plane surface, with some confidence that it will provide us with a good approximation to the contribution of the surface to the free energy of the cylinder. The surface layer occupies such a small proportion of the volume that we may calculate the magnetic contribution G_m by treating the surface current as though it flowed in a region indefinitely thin. Thus, $M = J/10$ emu,

$$F_m = (4\pi M)^2/8\pi,$$

and, per unit length of cylinder,

$$G = \pi R^2 F_m(J) + 2\pi R F_S(J).$$

The critical current J_C , corresponding to $G = 0$, is then given by

$$F_S(J_C) = -\frac{1}{2} R F_m(J_C).$$

The points in which the curves $F_S(J)$ and $-\frac{1}{2} R F_m(J)$ intersect determine the critical currents for the two senses of circulation about the axis of the cylinder, J_C^+ and J_C^- . However, when R is large, $|J_C^+| \approx |J_C^-| = J_C$, J_C is much smaller in magnitude than J_m^+ or J_m^- [the maximum surface currents for which solutions

to (1) and (2) can be found], and $F_S(J) \approx F(0)$ (see Fig. 1). Consequently in the large-radius limit the critical current J_C is given by

$$F_m(J_C) \approx -2F_S(0)/R. \tag{7}$$

In terms of the magnetization M , (7) can now be rewritten

$$4\pi M(R/2\lambda)^{1/2}/H_C = (-2h^{1/2}\varphi/\kappa)^{1/2} = \mu, \tag{8}$$

where μ is a parameter we shall need to refer to.

In the limit of high κ , φ becomes independent of κ and $\mu\sqrt{\kappa}$ is then a universal function of reduced field h . It is plotted against h in Fig. 2 for several values of κ , high as well as low. Notice how slowly $\mu\sqrt{\kappa}$ varies with κ except at low fields. In Fig. 3 we have plotted μ for a few values of κ in order to compare our results with the results of Fink and Barnes⁶ which were presented as a plot of $\mu\eta$ against h (η is a number ~ 1). For low values of κ a magnetic contribution to the surface free energy for zero current cannot be neglected though we have neglected it in the discussion above. It has been included as a correction term added to φ in (8) for the calculation of the curves in Figs. 2 and 3, and we have indicated in Fig. 3 how much difference this correction makes to $\mu(h)$ for one or two values of κ .

Our results would appear to differ from those of Fink and Barnes⁶ as a result of several approximations they make which become particularly poor at low κ and low h . In particular they neglect the minimization of free energy with respect to the vector potential \vec{A} [which

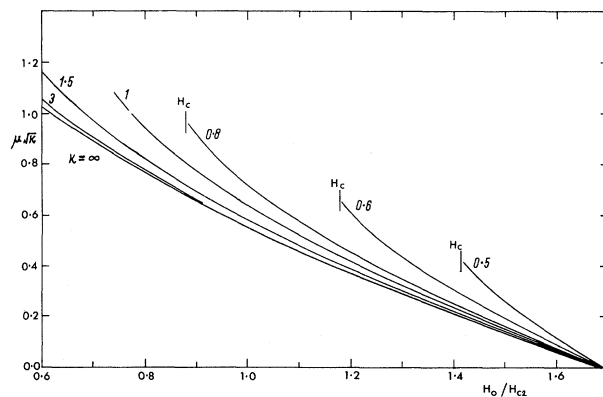


FIG. 2. The parameter $\mu\sqrt{\kappa} = 4\pi M(R/2\xi)^{1/2} H_C$ (where R is the radius of cylinder and $\xi = \lambda/\kappa$ is the coherence length) is plotted here against reduced field H_0/H_{C2} for several values of κ .

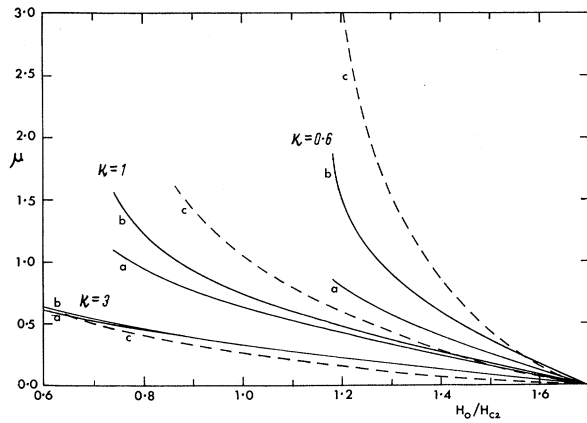


FIG. 3. Curves *a*: The parameter $\mu = 4\pi M(R/2\lambda)^{1/2} H_C$ is plotted against reduced field for three values of κ . Curves *b*: The same, but omitting the magnetic contribution to the surface free energy for zero current, which was added to φ as a correction term in computing curves *a* (see text). Curves *c*: The parameter $\mu\eta$ ($\eta \sim 1$) calculated by Fink and Barnes⁶ for the same values of κ as curves *a* and *b*.

leads to (2)].

When $\kappa > 0.707$ it will be noticed that we have presented results for μ and $\mu\sqrt{\kappa}$ both above and below H_{C2} . Above H_{C2} the criterion for the critical state $G = 0$ seems a plausible one, since our solutions describe states of the whole material. Below H_{C2} they do not. We have assumed, as in earlier calculations,^{8,9} that the surface solutions of the type described here ($f = 0$ as $x \rightarrow \infty$) are approximately valid below H_{C2} provided the field is near enough to H_{C2} for the average order parameter in the bulk of the material, which is in the mixed state, to be small. Since our solutions do not describe the state of the whole material, we cannot now expect $G = 0$, calculated neglecting the existence of the mixed state, to be the criterion for the critical state even if it is the correct criterion above H_{C2} . The results below H_{C2} must therefore be taken as a first approximation only.

Consider now the critical surface current of a rectangular foil when only the surface is superconducting and when the applied field H_0 is parallel to the surface but normal to the current—as it was assumed to be for the cylinder in the calculation above. But suppose now that the current is passed along the length of the specimen from an external source. In an earlier calculation⁸ we had assumed that the critical current was equal to the maximum current

for which solutions to the Ginzburg-Landau equations could be found (J_m^+ or J_m^- in Fig. 1). These currents are at least an order of magnitude higher than those generally observed,¹⁰ and Fink and Barnes⁶ have suggested that this may be due to the omission of the field energy, and not just to the imperfections of real surfaces. Here we adopt the same hypothesis as we have used above: that the critical state corresponds to $G = 0$, the Gibbs free energy in the superconducting state being calculated relative to the normal state carrying no current. We cannot justify this hypothesis since the normal state in the presence of the current is not in thermodynamic equilibrium, but we use it as the best guess we can make at present.

Now, whether the foil is normal or superconducting, if the total current per unit width of foil is J A/cm, the field on one side of the foil, assumed semi-infinite (except in thickness t), is $H_0 + 2\pi J/10$, while on the other the field is $H_0 - 2\pi J/10$. In the transition the field changes inside the material, but not outside it: In the surface superconducting state the field inside is equal to H_0 if both surfaces are superconducting (and carry equal currents), but $H_0 + 2\pi J/10$ if only one surface is superconducting, while in the normal state the field varies linearly across the thickness. In order to calculate the magnetic contribution to the free energy (3), we regard the superconductor as lying in the nonuniform field H_0' produced in the normal state by the currents supplied from external sources, one the specimen current, the other the current to the magnet producing H_0 . Thus, for example, when both surfaces are superconducting,

$$G_m = \int_{-\frac{1}{2}t}^{\frac{1}{2}t} \frac{(H_0 - H_0')^2 dx}{8\pi}$$

per unit area of foil. We then have the results that for a foil thick enough so that $t \gg \xi$, if $J_c(t)$ is the critical value of current per unit width of superconducting surface for a foil thickness t , and $M(R)$ the value of M for the cylinder radius R ,

$$J_c(t) = 10M(t/3) \text{ A/cm,}$$

when both surfaces are superconducting; if only one surface is superconducting (superconductivity having been destroyed on the other

by some means such as copper plating),

$$J_c(t) = 10M(2t/3) \text{ A/cm.}$$

According to these results the critical surface current of foils of a given material should vary at a given field and temperature as $t^{-1/2}$.

¹D. Saint James and P. G. de Gennes, Phys. Letters **7**, 306 (1963).

²D. P. Jones and J. G. Park, Phys. Letters **20**, 111 (1966).

³J. G. Park, Rev. Mod. Phys. **36**, 87 (1964).

⁴D. J. Sandiford and D. G. Schweitzer, Phys. Letters **13**, 98 (1964).

⁵M. A. R. LeBlanc, Phys. Letters **9**, 9 (1964); L. J. Barnes and H. J. Fink, to be published.

⁶H. J. Fink and L. J. Barnes, Phys. Rev. Letters **15**, 792 (1965).

⁷H. J. Fink, Phys. Letters **19**, 364 (1965).

⁸J. G. Park, Phys. Rev. Letters **15**, 352 (1965).

⁹H. J. Fink, Phys. Rev. Letters **14**, 309 (1965).

¹⁰P. S. Swartz and H. R. Hart, Jr., Phys. Rev. **137**, A818 (1965); I. P. Morton and J. G. Park, to be published; R. V. Bellau, to be published.

ELECTROREFLECTANCE IN METALS

J. Feinleib

Lincoln Laboratory,* Massachusetts Institute of Technology, Lexington, Massachusetts

(Received 27 May 1966)

Longitudinal electric field modulation of reflectivity has proven to be a powerful tool for investigating electronic band structure in semiconductors.^{1,2} In metals, the penetration of the low-frequency (<100-Hz) electric field was thought to be insufficient to produce an observable change in reflectivity. Nevertheless, we have observed electric field modulation of the reflectivity at a metal-electrolyte interface in several metals.

According to recent theories,^{1,3} electroreflectance depends on the influence of the low-frequency field on the energy bands, which causes an oscillating singularity at critical points.³ The relative change in the reflectivity at these singular-point energies should therefore depend on the magnitude of the electric field inside the solid within the penetration depth of the light. Using an electrolyte method,^{4,2} it is possible to obtain large fields at the sample surface with small applied voltages because a dipole layer is formed in the electrolyte at the interface. The penetration of the low-frequency field into the material is limited by the screening of the free carriers. The Thomas-Fermi screening length for a static charge in an electron gas is given as $\lambda^2 = \mathcal{E}_F / 6\pi n e^2$, where n is the carrier density, and \mathcal{E}_F is the Fermi energy. In semiconductors the screening length for the nearly static field can be of the order of the wavelength of the light, but in good conductors the screening occurs within atomic dimensions of the surface, leaving a field-free region in the bulk of the metal. In copper, for example,

the screening length $\lambda \approx 0.5 \times 10^{-8} \text{ cm} \approx 0.5 \text{ \AA}$. The electric field should therefore have little effect on the band structure at the depth that is probed by the light which is of the order of 100 \AA . Despite these considerations, in the metals examined to date, silver, gold, copper, and the metallic-oxide sodium tungsten bronze,⁵ peaks in the electroreflectivity spectra have been observed which are closely correlated with structure in the reflectivity of each metal. The relative change in reflectivity at the strong peaks was about 0.5% which is comparable with the electroreflectance structure observed in semiconductors.²

The experimental arrangement is similar to the electrolyte technique used for studying semiconductors.² The metal sample is placed in a fused-quartz cell at the entrance slit of a single-pass Perkin-Elmer prism monochromator and is illuminated by a 1600-W xenon arc source. A 35-Hz modulating voltage of about 2 V peak to peak is applied between the sample and a platinum electrode which are immersed in the KCl-water electrolyte. No dc bias voltage was required. The detectors used are photomultiplier tubes with responses from about 1.3 to 6.0 eV. Most of the structure in the electroreflectance is observable with moderate resolution, using slit widths of 100 μ and a CaF_2 prism for the ultraviolet or a glass prism for the visible spectrum. The photomultiplier output detected at the 1000-Hz chopper frequency is kept constant over the spectral range by a servo control